Title: Long-Wavelength Reflecting Filters Found in the Larval Retinas of One Mantis Shrimp Family (Nannosquillidae)

Authors: Kathryn D. Feller[1,2,3*], David Wilby[3,4], Gianni Jacucci, Silvia Vignolini, Judith Mantell[5], Trevor J. Wardill[1,2], Thomas W. Cronin[5], Nicholas W. Roberts[3].

Affiliations:

[1] University of Minnesota, Ecology, Evolution and Behavior Department, 1479 Gortner Avenue, St. Paul, Minnesota, 55108 USA

[2] University of Cambridge, Physiology Development and Neuroscience Department, Physiological Laboratories, Downing Street, Cambridge, CB2 3EG, United Kingdom.

[3] University of Bristol, School of Biological Sciences, Life Sciences Building, 24 Tyndall Ave, Bristol, UK, BS8 1TQ.

[4] Lund University, Department of Biology, Lund, 223 62, Sweden

[5] University ---of Bristol, Wolfson Bioimaging Facility, Biomedical Sciences Building, University Walk, Bristol, UK, BS8 1TD

[6] University of Maryland Baltimore County, Department of Biological Sciences, 1000 Hilltop Circle, Baltimore, Maryland 21250 .

*Correspondence to: kate.feller@gmail.com

Abstract: Here we describe a new type of optical feature, discovered in the eyes of stomatopod (mantis shrimp) crustacean larvae. Each rhabdom, or photoreceptor, in these larval retinas are bisected into a distal and proximal tier by a photonic crystalline structure, similar to the intrarhabdomal filters known from adult stomatopods. Unlike the adults, however, our histological examinations of larval eyes demonstrate that each intrarhabdomal photonic crystal (IPC) contains a 3-dimensional, ordered array of membrane-bound vesicles, each approximately 155 nm in diameter. The most unique feature of the IPC is its ability to reflect a narrow band of long-wavelength light (average reflectance max, 572 nm) when illuminated with on-axis light *in vivo*. The discovery of this novel reflecting structure redefines our understanding of visual tuning via optical filters, previously assumed to only provide filtering by light absorption. IPCs provide the first example that filters may tune vision by filtering *and* reflection. Further, IPC structures were only found in the retinas of species from the same closely related family, Nannosquillidae. Since these larvae co-occur with other species of stomatopod larvae that lack IPC structures in their retinas, this poses and interesting case for the evolution of IPC structures as well as the broader evolution of crustacean visual systems.

One Sentence Summary photonic crystal

This study describes a novel photonic structure within the photoreceptors of stomatopod (mantis shrimp) larvae that redefines our understanding of how optical structures may be used to tune visual sensitivities.

Main Text

Introduction: Optical features are commonly used to tune animal visual systems. Many species of both vertebrates and invertebrates use a reflecting structure, or tapetum, behind their photoreceptors to improve vision in dim light (*1-4*). Others use colorful filters positioned either around or over their photoreceptors to tune their spectral sensitivity by absorbing specific

wavelengths of light (*5*-*7*). We present a new type of optical structure that uses both properties of reflection and filtering to tune a visual system, discovered in the eyes of larval mantis shrimp crustaceans. These intrarhabdomal photonic structures (IPCs) are like a tapetum in that they use an assembly of ordered, photonic-sized structures to reflect light. Their location *within* the photoreceptors, however, provides selective reflection of a narrow band of long-wavelength light onto the photoreceptors *above* the IPC, while simultaneously filtering light that reaches the photoreceptors *below* the crystal, all in the absence of photostable pigments. The discovery of these optical structures challenges our assumption of how visual systems evolve within a lineage to meet the sensory needs of their users.

Adult mantis shrimp, or stomatopods, are benthic marine crustaceans famous for their elaborate and specialized eyes (*5*, *8*, *9*); execution of ultra-fast, power-amplified movements (*10*-*12*); and expression of multiple anatomical structures with unique materials properties (*13*-*16*). The breadth of unique discoveries made from stomatopod research provides biological inspiration on multiple applied technological fronts, including color and polarization cameras (*17*-*19*) and impact resistant materials
(*20*). Here we present a previously undescribed type of photonic structure found in stomatopods – though not in adults, but rather in the eyes of the larvae. Since stomatopod larvae are adapted for survival as plankton in the open ocean, they lack most of the adult visual attributes, such as colorful intrarhabdomal filters (*21*, *22*), fluorescent UV filters (*23*, *24*), massive visual pigment diversity (*5*, *9*, *25*), and specializations for linear and circular polarized vision

(*26*-*28*) and communication (*13*, *16*, *29*, *30*). Instead, hallmark features of stomatopod larvae include compound eyes with a single photoreceptor type (*31*-*33*); morphological adaptations for hiding in open-water, such as highly transparent bodies and reflective eye camouflage (*34*-*36*); and performance of daily migrations through the water column where they rise from the depths at night to hunt near the surface in a lunar dependent fashion (*37*, *38*). Our close examination of stomatopod larval eyes, facilitated by DNA barcoding (*38*), revealed the discovery of highly unusual IPC structures that are unlike any optical structures known from any other animal eyes or other tissues. Further, these IPC structures were only found in five species, all of which are members of the same closely related family, Nannosquillidae. Provided here is a description of the anatomical and optical properties of these photonic structures and an evaluation of the current evidence that may explain their biological function and evolution.

Novel photonic structures

All taxa of stomatopod larvae are understood to possess a pair of complex compound eyes composed of several hundred ommatidial units, each using transparent, apposition optics to focus light onto the photoreceptive rhabdom (*39*, *40*). The rhabdom is formed from visual pigment-expressing microvilli projected from a ring of seven retinular cells (R1-7). Screening pigments optically isolate each rhabdom from its surrounding neighbors, while reflective structures lie on the surface of the retina, between ommatidia, to camouflage the dark eye in open water (*34*). While the majority of stomatopod larval retinas adhere to this typical arrangement, we show that species from the family Nannosquillidae possess a conspicuous alteration. Located at approximately one-third the length of the rhabdom from the distal end lies

a barrel-shaped structure formed from four, equally proportioned cells (Figure 1). These four cells contains thousands of highly ordered, spheroid-shaped vesicles, each an average of 155 nm (±6.8 nm) in diameter. Transmission electron microscopy (TEM) and electron tomography reveal that the order of these vesicles is preserved across the membranes of the four primary cells (Figure 1D) and in three dimensions (S.Video 1). Each IPC structure measures an average of 11 μm (± 1.6 μm) long by 4.8 μm (± 1 μm) wide and lies directly in the optical pathway of light, bisecting the retinular cells (R1-7) of the rhabdom into a proximal (R2, R3, R6, & R7) and distal tier (R1, R4, & R5, Fig 1) in a similar pattern to the tiered rhabdoms found in the specialized color vision receptors of adult stomatopod eyes
(*26*). IPC structures were found in five, closely related species of nannosquillid larvae and do not vary significantly in their dimensions among species (S.Figure 1). The IPC structures were also found in different developmental stages, including the first and terminal stage, suggesting that the optical function is conserved throughout the entire pelagic phase of life.

Electron and light microscopy also reveal that IPC-expressing ommatidia are not uniformly expressed across the eye, but regionalized to the ventral and lateral retina (Figure 2). A subset of 40-50 ommatidia in the dorsal region of the eye are devoid of IPC structures and instead present the seven-retinular cell, ring structure typical of non-nannosquillid larvae (Figure 1C, 2D). Two-photon microscopy further established the three-dimensional distribution of IPC expressing and non-expressing ommatidia across the nannosquillid eye (Figure 2A-C, S.Video 2 & 3). This region of the eye may be for viewing a restricted region of the underwater light enviornment, such as the 97˚ window of light entering the water from the air, or Snell's Window.

IPC Interaction with Light

The size and arrangement of vesicles within the IPC structures led us to hypothesize that IPC structures may reflect light onto the overlying distal tier of the rhabom. To investigate how light interacts with the IPC, we designed a custom microscope system to illuminate, image, and measure reflected light from the pseudopupils of larval ommatidia *in vivo* (S.Figure 2). The pseudopupil, or dark spot that dances across the surface of a compound eye as it rotates (S.Video 4), is observed when the optical axes of a subset of ommatidia align with the optical viewing axis of an observer. Since the IPC lies in the optical axis, we predicted a distinct reflection would be observed when light was imaged down the pseudopupil of IPC-containing rhabdoms. This experiment was conducted blind to species identity by using wild-captured larvae identified via DNA barcoding *post hoc* of light reflectance measurements (*38*). In some larvae, a sharp reflectance of yellow light with an average peak of 572 nm was measured from ventral and lateral ommatidia only when illuminated on-axis (Figure 3). While side-illumination was sufficient to visualize and measure the blue and green camouflage structures that lie over the pigmented retina (*34*), only on-axis, epi-illumination could produce a yellow reflectance from the pseudopupil (S.Video 4). DNA barcoding revealed that yellow pseudopupil reflectances were only measured from nannosquillid specimens (Figure 3F). TEM verified the presence of IPC structures in these specimens (Figure 2), concluding that IPC structures were the source of observed yellow reflectances. This conclusion was bolstered by similar patterns of regionalization across the ventral and lateral retina for yellow reflectance and presence of IPC

structures (Fig 2A-D, Fig 3). Neither yellow reflectances, nor IPCs were found in the dorsal most ommatidia.

The tiered rhabdoms of adult stomatopods are spectrally tuned by the selective absorption by colored filters positioned at the distal ends of each tiered rhabdom (*22*). Unlike the intrarhabdomal filters of adults, we found no evidence of photostable filtering pigments inside the IPCs of tiered larval photoreceptors. Thus, filtering is primarily achieved by the coherent reflectance of wavelengths that interact with the structure, rather than by absorption of wavelengths by photostable pigments. Though the intrarhabdomal structures in adult versus larvae use very different optical properties to provide visual tuning to the photoreceptors, the location of these structures within tiered rhabdoms suggest they may share similar developmental origins.

To understand the origin of the wavelength-selective response observed from the pseudopupil we developed a semi-analytical model. This mathematical model uses a combination of Bragg's law (*41*) with finite distance time domain (FDTD) numerical simulations. By using these methods we were able to account for conditions of the *in vivo* experiment and morphological disorder of the IPC. Morphological disorder and periodicity of the vesicles was determined by calculating the structure factor, which is related to the Fourier transform of the vesicle positions measured from TEM micrographs (S. Equation 1). The structure factor of the vesicles within the IPC structure is related to a face centered cubic (FCC) geometry of the vesicles with an estimated lattice constant of 392 ±7 nm (Figure 4a; S.Figure 3a).

We found that our model is in good agreement with the experimental data after standardizing the predicted spectrum with a similar diffuse white light reference to the reflectance experiment,. This provides further evidence that the observed yellow reflectance measured from the larval pseudopupil is produced by the IPC (Figure 4b). The residual difference between the reflectivity of our predicted and observed reflectances can be attributed to several factors including potential histological distortion of IPC size (S.Figure 3d); unknown identities (and thus refractive indices) of vesicle and matrix materials; and additional disorder in the orientation and periodicity of the 3D lattice across large volumes outside the range of TEM tomography. All three of these factors are good targets for future investigations into the material properties of these unusual visual structures.

Discussion

The discovery of IPC structures raises three major questions. First, what source of light is available in the natural habitat of nannosquillid larvae to interact with the IPCs? We have established that when the IPC interacts with white light, it maximally reflects a narrow band of long-wavelengths that peak around 572 nm. Since stomatopod larvae are active in the nocturnal pelagic habitat there are only a few sources of long-wavelengths to consider. The irradiance spectrum of moonlight possesses long-wavelengths, however these wavelengths would only be abundant close to the surface and during periods of the full moon since they are heavily filtered and scattered within several meters of depth. It is unlikely that nannosquillid visual systems would be tuned to interact with the wide-field, long-wavelength components of moonlight since

these larvae are not typically captured near the surface during the full moon, only during the quarter and dark phases (pers. observ; pers com RL Caldwell). The only other source of long-wavelengths found in the nocturnal, pelagic habitat is bioluminescence. Though most bioluminescence emission spectra peak in the short-wavelength, blue range (480 nm, (*42*), many coastal species that overlap in habitat with stomatopod larvae have red-shifted emission spectra with emission tails into the long-wavlength range (>540nm; (*42*, *43*). The lack of moonlight from the depth and time at which nannosquillid larvae are actively foraging suggests that bioluminescence is the most likely source of long-wavelengths that interact with IPC reflectors. It is perhaps the case that the dorsal region of the eye, lacking IPC structures, may be for looking upwards for non-luminescent objects against a wide-angle field of illumination, whereas the lateral and ventral regions of the eye uses IPC-containing ommatidia facilitate imaging point sources of bioluminescent light around and below the animal, as is known for some mesopelagic species (*40*).

If coastal bioluminescence is the most likely illumination source interacting with IPC structures, it then raises the second question: How does the IPC affect nannosquillid larval vision? Yellow caretenoid pigmentations are known filters for tuning both terrestrial (*44*) and deep sea (*45*, *46*) visual systems to bioluminescent sources. Given the hypothesized relationship between bioluminescent light sources and the yellow-reflecting IPC structures, we developed a mathematical model to test how IPC filtering/reflectances may impact the photon capture (quantal catch) in each photoreceptive tier (based on *47*). This model incorporated the reflectance and morphological measurements reported from our experiments with digitized, red-shifted bioluminescent emission spectra from the literature (*48*) and known visual pigments from nannosquillid larvae (*32*, *49*). In short, the model generates a range of estimated bioluminescence spectra, each peaking in a range from 450nm to 650nm; at each of these peak emission spectra, the model calculates the number of photons captured by an ommatidium with and without an IPC (Figure 4). The specifics of these calculations and the data used to build the mathematical model are reported in the Supplemental Materials. The model output demonstrates that long-wavelength photons are captured at a greater rate with the addition of an IPC, but only in the presence of a visual pigment with an absorption probability (λ_{max}) greater than 500 nm (Figure 4). Since the longest-wavelength visual pigment measured from nannosquillid larvae is λ_{max} 504 nm, it is likely that the IPC aids to improve the ability of the distal tier to absorb long-wavelength light present in the nocturnal pelagic habitat. The model predicted no effect, either from IPC filtering or reflectance, on photoreceptors that contain visual pigments with λ_{max} shorter than 500 nm. Since most visual models of bioluminescence are calculated for vision in the deep sea (*50*-*54*), our model is the first to attempt to characterize a system for bioluminescence detection in the nocturnal pelagic habitat near the surface, where the background is not total darkness. To properly address the impact of IPCs on visual performance, such as contrast sensitivity, further experiments are warranted to quantify the spectral sensitivity of each photoreceptive tier in IPC-containing retinas as well as the bioluminescent emission spectra from species sympatric to nannosquillid larvae.

The third question raised by the discovery of IPC retinas is its expression in larvae of a single, closely related family of stomatopod species, the Nannosquillidae. The nannosquillid individuals

included in our experiments were captured and tested alongside seven additional stomatopod species, none of which contain IPC structures in their retinas. The nannosquillid larvae are the first of *any* described crustacean larvae (decapod, stomatopod) to present a specialized photoreceptor array differing from the canonical larval retina structure (*31*, *33*). Currently, we can only speculate the behavioral consequences and pressures that selected evolution of this optically sophistocated system. It is possible that IPC structures evolved to allow nannosquillid larvae to prey upon bioluminescent targets, allowing them to occupy a discrete predatory niche within the zooplanktonic environment relative to other larvae. However, this system is just as likely to provide anti-predation measures for spotting large, planktivorous predators that produce bioluminescence intrinsically or in their wake (*55*). Visualization of bioluminescence may also serve as a coastal 'proximity detector' to help maintain the larvae's position near the adult settlement habitat in the intertidal zone. Regardless of the specific role IPC structures play in tuning vision to these animals' ecology, we provide compelling evidence that within the stomatopod lineage, the nannosquillids are experiencing a markedly different sensory evolution from the majority of the stomatopod order. No larger than a grain of rice, these wee beasts provide a totally new photonic mechanism for biological interactions with light.

Contributions

Initial discovery, development, and orchestration of research conducted by KDF under the mentorship of TWC and NWR. TEM done by KDF and JM; optical modeling performed by DW; and 2-photon microscopy executed by TJW. Text and figures composed by KDF with additions by DW and revisions by co-authors.

Acknowledgments

Funding for this work was provided from the US Air Force Office of Scientific Research; Australian Microscopy and Microanalysis Research Facility Travel and Access Program Grant Special thanks for help with the to Megan L Porter, Roy L Caldwell, Justin Marshall, Elliott P. Steele, Sitara Palecanda, John Cataldi, Sonke Johnsen, Tom Jordan, Chere Petty, Lindsdey DeMelo and the Marine Resources Center at the Marine Biological Laboratory, the UMBC Porter Imaging Facility, and the Australian Museum's Lizard Island Research Station, run by Lyle Vale and Anne Hoggart.

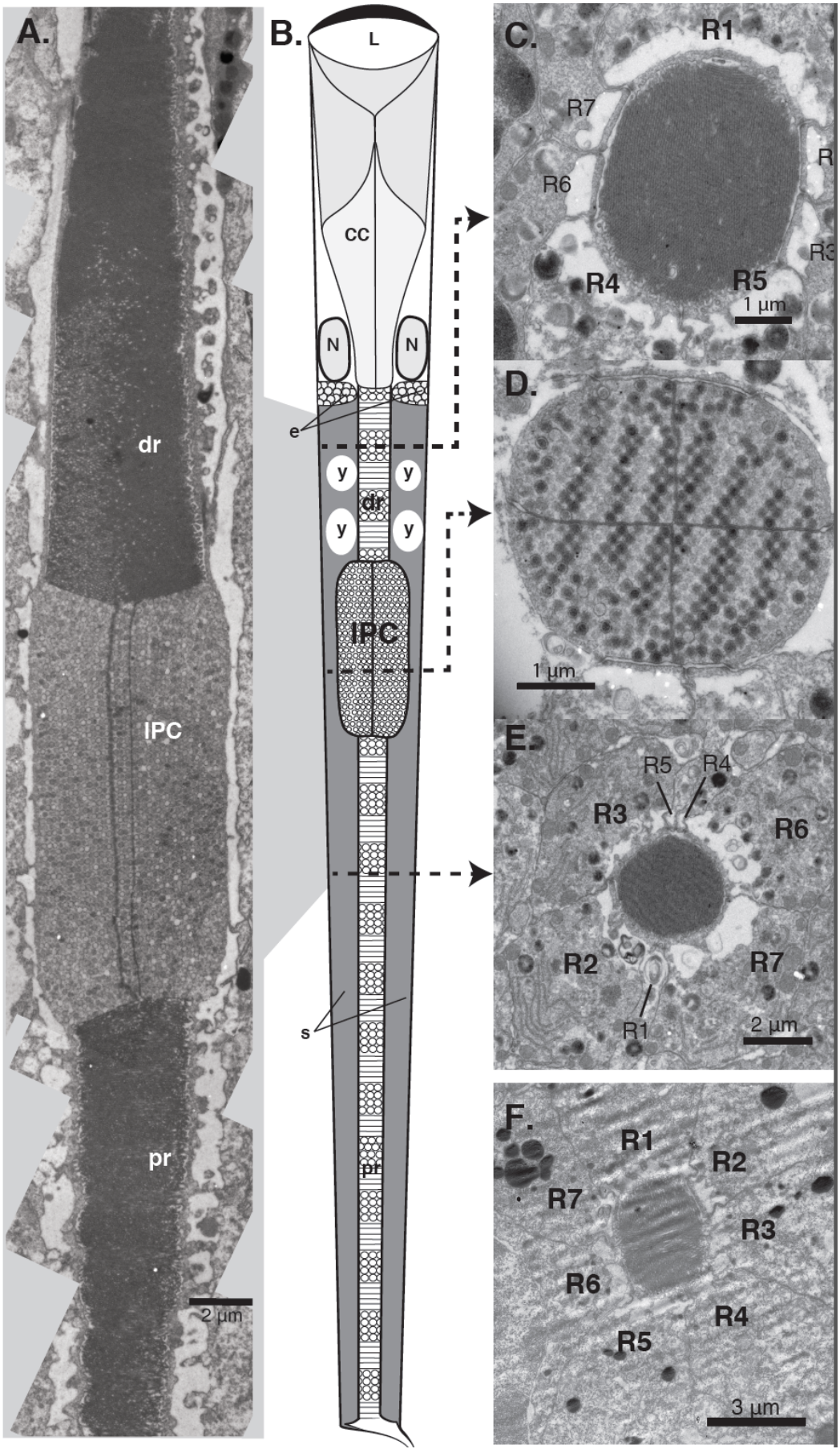
A.
dr
IPC
pr
2 µm
B.
L
cc
N
N
e
y
y
y
y
dr
IPC
s
pr
C.
R1
R7
R6
R
R3
R4
R5
1 µm
D.
1 µm
E.
R5
R4
R3
R6
R2
R7
R1
2 µm
F.
R1
R2
R7
R3
R6
R4
R5
3 µm

Figure 1 Anatomy of stomatopod larval ommatidia containing intrarhabdomal photonic structures (IPC) (A) Composite TEM of longitudinal section through the ommatidium. Microvilli in the distal (dr) and proximal (pr) rhabdoms flank the IPC. (B) Diagram showing the anatomical organization of an IPC containing ommatidium. (C) TEM cross-section through the distal tier of the rhabdom, formed by microvilli from retinular cells R1, R4, and R5 (nomenclature from (*22*). As with adult tiered rhabdoms, extensions of the remaining retinular cells are visible, however they do not contribute microvilli to the rhabdom (D) TEM cross-section through the IPC, which is composed of four equally proportioned cells and contains a crystalline lattice of vesicles, the order of which is preserved in 3 dimensions across the membranes of the four primary cells. Dark banding patterns are an artifact of uptake of stain consistent with TEM images of other clear vesicle structures (*56*). (E) TEM cross-section through the proximal rhabdomeric tier, formed by microvillar projections from retinular cells R2, R3, R6 and R7. (F) TEM Cross-section through a non-IPC expressing photoreceptor in the dorsal region of the eye. Note the equal contribution of microvilli from retinular cells R1-7. Lens, L; crystalline cone, CC; Retinular cell nucleus, N; reflective eye camouflage, e; yellow, long-pass screening pigments, y; lateral screening pigments, s.

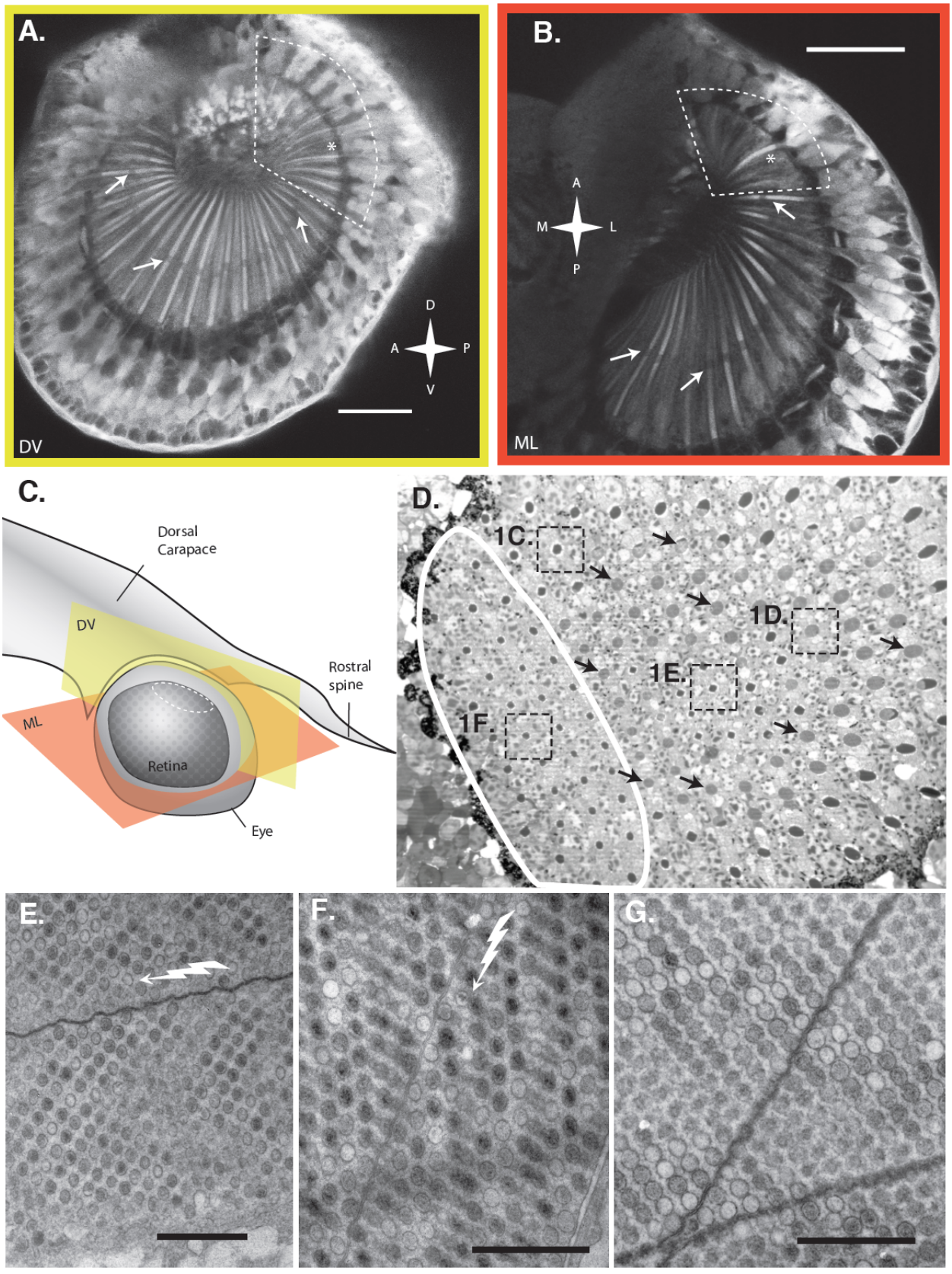
A.
DV
D
A
P
V
B.
ML
A
M
L
P
C.
Dorsal
Carapace
DV
Rostral
spine
ML
Retina
Eye
D.
1C.
1D.
1E.
1F.
E.
F.
G.

Figure 2 Regional expression of IPCs across the retina and in the eyes of five different nannosquillid species and developmental stages. (A-B) Two-photon optical sections of *Coronis scolopendra* first stage larval eyes revealing a small region of dorsal pointing ommatidia (within dotted line) lacking IPC structures (denoted by *). Arrows indicate a subset of IPC structures in each section. Compasses orient anatomical directions: A, anterior, P, posterior, M, medial, L, lateral, D, dorsal, V, ventral. Scale bars, 50 μm (C) Diagram of dorsal-ventral (DV) and medial-lateral (ML) sections through eye in A and B, respectively. (D) Light micrograph of retina cross-section from early stage larva, unknown nannosquillid species. Boxes depict regions imaged via TEM in figure 1C-F. White line denotes dorsal region of untiered ommatidia lacking IPC expression, similar to zone identified in A-C. Arrows highlight subset of IPC structures in the remainder of the eye. (E) TEM longitudinal section of IPC in last stage larva, *Pullosquilla thomassini* and (F) mid stage *Alachosquilla vicina.* Jagged arrows indicate direction of incoming light. (G) Oblique TEM section of IPC in early stage, *Pullosquilla litoralis* larva. E-G scale bars, 1 μm.

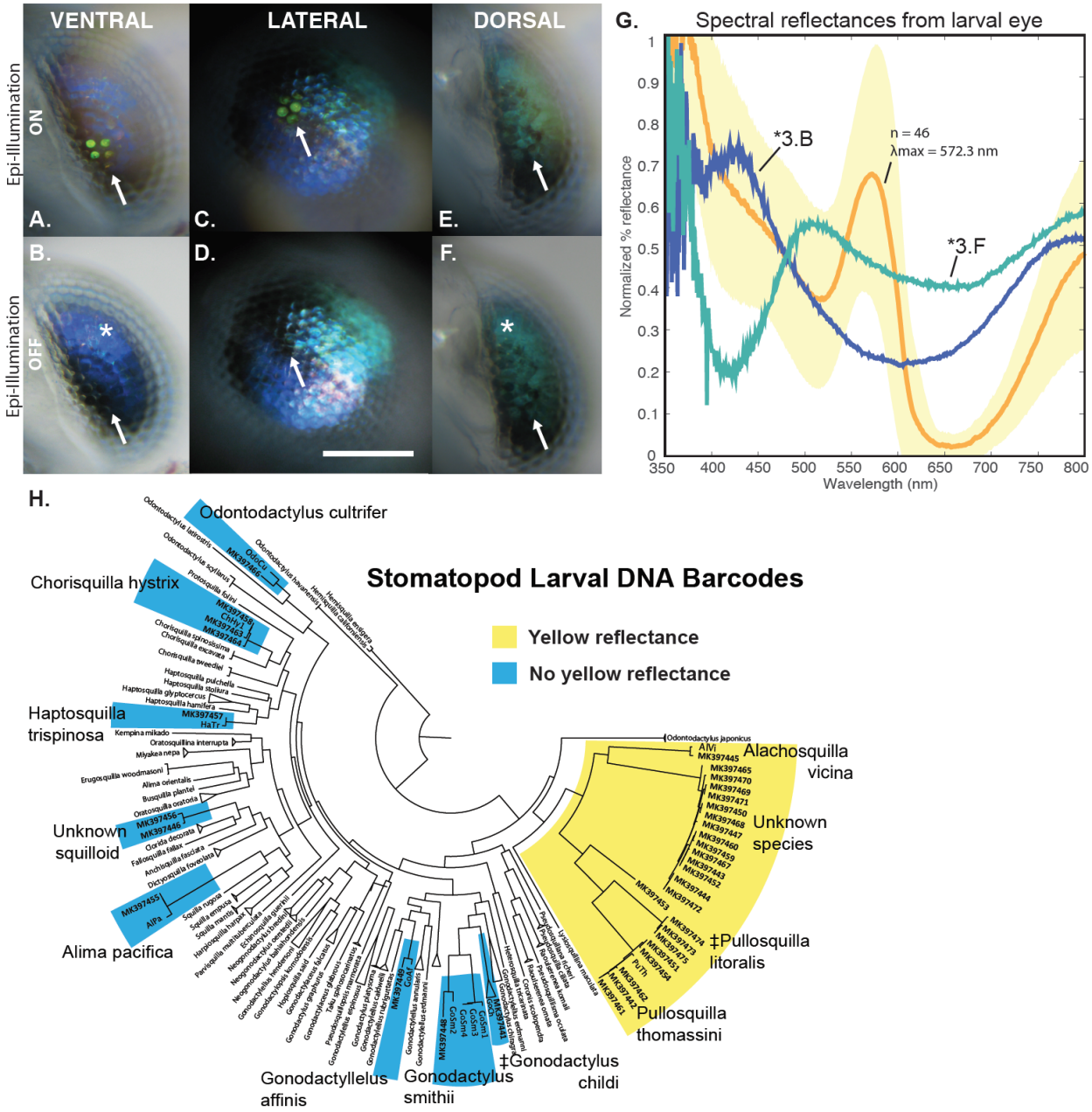

Figure 3 *In vivo* illumination of the pseudopupil with on-axis light (epi-illumination) reveals a sharp, yellow reflectance from IPC expressing ommatidia only in nannosquillid larvae. (A-F) Illumination of a single nannosquillid eye from three directions with epi-illumination on or off. The only condition varied between each pair of ventral, lateral, or dorsal images is the state of the epi-illuminated light (on or off; as in SV5). White arrows indicate pseudopupil. Side-illumination was used to illuminate the entire eye for communication purposes and was removed during spectral measurements. The dorsal region of the eye does not produce a yellow reflectance, E, which corresponds to an absence of IPC structures. Scale bar = 150 μm for all images. (G) On-axis illumination normalized reflectance spectra measured from photonic structures depicted in A-F. Blue and green lines, eye camouflage reflectances from regions denoted in B and F by *. Yellow line represents average pseudopupil reflectance from 46 nannosquillid pseudopuils, which

peaks at 572.3 nm. Yellow shading, standard error of pseudopupil reflectance measurements. Yellow reflectance corresponds to yellow pseudopupils in A and C. (H) Maximum likelihood tree of DNA barcodes from adult references and larval sequences from individuals sampled in epi-reflectance experiment. Sequences highlighted in yellow indicate larvae in which a yellow pseudopupil reflectance was measured. Sequences highlighted in blue represent larval eyes that did not produce yellow reflectances. The yellow highlighted clade also corresponds to the Nannosquillidae family. ‡ indicate species where reflectance was not measured, but IPC absence or presence was determined via TEM only.

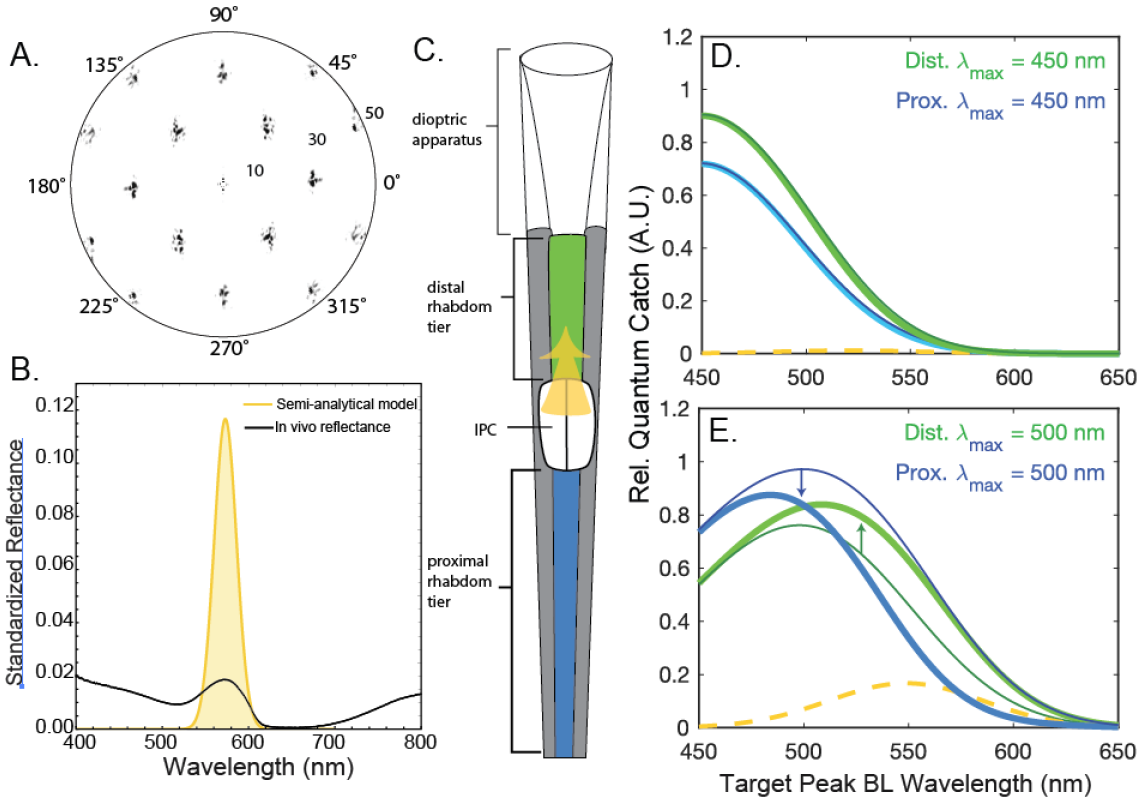

Figure 4. Results of models for IPC photonic mechanism and quantum catch (QC) with and without IPC structures. (A) Two-dimensional structure factor unveiling the FCC packing of the vesicles in the IPC. (B) Comparison between the optical response of the IPC predicted by our semi-analytical model and the experimental data, yellow and black curve, respectively. Our model proves that the observed wavelength-selective response is caused by the IPC. (C) Diagram depicting the morphology of a single IPC containing ommatidium. Colors correspond to quantal traces in D and E. (D-E) Relative Quantal catch calculated for bioluminescent emission spectra peaking at each wavelength between 450nm and 650nm in proximal and distal photoreceptive tiers with 450nm (D) or 500nm (E) peak absorbing (λ_{max}) visual pigments. Thin, dark solid lines show the QC in each tier in the absence of the IPC reflectance; thick lines show the QC in each tier when reflection from the IPC is added; dashed yellow lines show the amount of QC in the distal tier accounted for from IPC reflection alone. Arrows indicate the change in QC of a given tier with the addition of an IPC Note how IPC reflectance only affects QC of photoreceptors expressing 500 nm visual pigment.

References

1. E. R. Loew, Light, and photoreceptor degeneration in the Norway lobster, Nephrops norvegicus (L.). *Proceedings of the Royal Society of London. Series B, Biological Sciences*. **193**, 31–44 (1976).

2. E. J. Warrant, P. D. McIntyre, Strategies for retinal design in arthropod eyes of low F-number. *Journal of Comparative Physiology A: Neuroethology, Sensory, Neural, and Behavioral Physiology*. **168**, 499–512 (1991).

3. X. Qiu, K. Vanhoutte, D. Stavenga, K. Arikawa, Ommatidial heterogeneity in the compound eye of the male small white butterfly, Pieris rapae crucivora. *Cell Tissue Res*. **307**, 371–379 (2002).

4. B. A. Palmer *et al.*, Optically functional isoxanthopterin crystals in the mirrored eyes of decapod crustaceans. *Proceedings of the National Academy of Sciences of the United States of America*. **115**, 2299–2304 (2018).

5. T. W. Cronin, M. J. Bok, N. J. Marshall, R. L. Caldwell, Filtering and polychromatic vision in mantis shrimps: themes in visible and ultraviolet vision. *Philosophical Transactions of the Royal Society of London. Series B: Biological Sciences*. **369**, 20130032–20130032 (2014).

6. D. G. Stavenga, B. D. Wilts, Oil droplets of bird eyes: microlenses acting as spectral filters. *Philosophical Transactions of the Royal Society of London. Series B: Biological Sciences*. **369**, 20130041–20130041 (2014).

7. K. Arikawa, D. Stavenga, Random array of colour filters in the eyes of butterflies. *Journal of Experimental Biology*. **200**, 2501–2506 (1997).

8. H. H. Thoen, M. J. How, T. H. Chiou, J. Marshall, A Different Form of Color Vision in Mantis Shrimp. *Science*. **343**, 411–413 (2014).

9. J. Marshall, T. Cronin, S. Kleinlogel, Stomatopod eye structure and function: A review. *Arthropod Structure and Development*. **36**, 420–488 (2007).

10. S. N. Patek, M. V. Rosario, J. R. A. Taylor, Comparative spring mechanics in mantis shrimp. *Journal of Experimental Biology*. **216**, 1317–1329 (2013).

11. S. N. Patek, R. L. Caldwell, Extreme impact and cavitation forces of a biological hammer: strike forces of the peacock mantis shrimp Odontodactylus scyllarus. *The Journal of Experimental Biology*. **208**, 3655–3664 (2005).

12. S. N. Patek, W. L. Korff, R. L. Caldwell, Biomechanics: deadly strike mechanism of a mantis shrimp. *Nature*. **428**, 819–820 (2004).

13. T. H. Chiou, A. R. Place, R. L. Caldwell, N. J. Marshall, T. W. Cronin, A novel function for a carotenoid: astaxanthin used as a polarizer for visual signalling in a mantis shrimp. *The Journal of Experimental Biology*. **215**, 584–589 (2012).

14. J. C. Weaver *et al.*, The Stomatopod Dactyl Club: A Formidable Damage-Tolerant Biological Hammer. *Science*. **336**, 1275–1280 (2012).

15. N. Roberts, T. Chiou, N. Marshall, T. Cronin, A biological quarter-wave retarder with excellent achromaticity in the visible wavelength region. *Nature Photonics* (2009).

16. T. M. Jordan *et al.*, A shape-anisotropic reflective polarizer in a stomatopod crustacean. *Nature Publishing Group*, 1–8 (2016).

17. M. Garcia, T. Davis, S. Blair, N. Cui, V. Gruev, Bioinspired polarization imager with high dynamic range, 1–7 (2018).

18. M. Garcia, C. Edmiston, R. Marinov, A. Vail, V. Gruev, Bio-inspired color-polarization imager for real-time in situ imaging. *Optica*. **4**, 1263–9 (2017).

19. T. York *et al.*, Bioinspired Polarization Imaging Sensors: From Circuits and Optics to Signal Processing Algorithms and Biomedical Applications. *Proc. IEEE*. **102**, 1450–1469 (2014).

20. L. Grunenfelder *et al.*, Bio-inspired impact-resistant composites. *Acta Biomaterialia*. **10**, 3997–4008 (2014).

21. T. Cronin, N. Marshall, R. Caldwell, The intrarhabdomal filters in the retinas of mantis shrimps. *Vision Research*. **34**, 279–291 (1994).

22. N. J. Marshall, M. F. Land, C. A. King, T. W. Cronin, The Compound Eyes of Mantis Shrimps (Crustacea, Hoplocarida, Stomatopoda). II. Colour Pigments in the Eyes of Stomatopod Crustaceans: Polychromatic Vision by Serial and Lateral Filtering. *Philosophical Transactions of the Royal Society B: Biological Sciences*. **334**, 57–84 (1991).

23. M. J. Bok, M. L. Porter, T. W. Cronin, Ultraviolet filters in stomatopod crustaceans: diversity, ecology and evolution. *Journal of Experimental Biology*. **218**, 2055–2066 (2015).

24. M. J. Bok, M. L. Porter, A. R. Place, T. W. Cronin, Biological Sunscreens Tune Polychromatic Ultraviolet Vision in Mantis Shrimp. *Current Biology*. **24**, 1636–1642 (2014).

25. M. L. Porter, M. J. Bok, P. R. Robinson, T. Cronin, Molecular diversity of visual pigments in Stomatopoda (Crustacea). *Visual neuroscience*. **26**, 255–265 (2009).

26. N. J. Marshall, M. F. Land, C. King, T. W. Cronin, The Compound Eyes of Mantis Shrimps (Crustacea, Hoplocarida, Stomatopoda). I. Compound Eye Structure: The Detection of Polarized Light. *Phil Trans R Soc Lond B*. **334**, 33–56 (1991).

27. T.-H. Chiou *et al.*, Circular Polarization Vision in a Stomatopod Crustacean. *Current Biology*. **18**, 429–434 (2008).

28. I. M. Daly *et al.*, Dynamic polarization vision in mantis shrimps. *Nature Communications*. **7**, 1–9 (2016).

29. M. J. How *et al.*, Out of the blue: the evolution of horizontally polarized signals in Haptosquilla (Crustacea, Stomatopoda, Protosquillidae). *Journal of Experimental Biology*. **217**, 3425–3431 (2014).

30. T. Cronin *et al.*, Polarization vision and its role in biological signaling. *INTEGR. COMP. BIOL*. **43**, 549 (2003).

31. T. Cronin, R. Jinks, Ontogeny of Vision in Marine Crustaceans. *American Zoology*. **41**, 1098–1107 (2001).

32. K. D. Feller, T. W. Cronin, Spectral absorption of visual pigments in stomatopod larval photoreceptors. *Journal of Comparative Physiology A: Sensory, Neural, and Behavioral Physiology*. **202**, 215–223 (2016).

33. T. W. Cronin, M. J. Bok, C. Lin, Crustacean Larvae—Vision in the Plankton. *INTEGR. COMP. BIOL*, 1–12 (2017).

34. K. D. Feller, T. W. Cronin, Hiding opaque eyes in transparent organisms: a potential role for larval eyeshine in stomatopod crustaceans. *Journal of Experimental Biology*. **217**, 3263–3273 (2014).

35. C. Haug, J. T. Haug, Defensive enrolment in mantis shrimp larvae (Malacostraca: Stoamtopoda). *Contributions to Zoology*. **83**, 185–194 (2014).

36. C. Haug, S. T. Ahyong, J. H. Wiethase, J. Olesen, J. T. Haug, Extreme morphologies of mantis shrimp larvae. *Nauplius*. **24**, 185–15 (2016).

37. J. Ohtomi, H. Kawazoe, T. Furota, Larval stage composition and morphological change during larval development of the Japanese mantis shrimp, Oratosquilla oratoria (De Haan, 1844)(Stomatopoda, Squillidae) in Tokyo Bay, Japan. *Crustaceana*. **78**, 1325–1337 (2005).

38. K. D. Feller, T. W. Cronin, S. T. Ahyong, M. L. Porter, Morphological and molecular description of the late-stage larvae of Alima Leach, 1817 (Crustacea: Stomatopoda) from Lizard Island, Australia. *zootaxa*. **3722**, 22–32 (2013).

39. D. Nilsson, Evolutionary links between apposition and superposition optics in crustacean eyes. *Nature*. **302**, 818–821 (1983).

40. D.-E. Nilsson, in *Zooplankton: sensory ecology and physiology*, P. H. Lenz, D. K. Hartline, J. E. Purcell, D. L. Macmillan, Eds. (Gordon and Breach, 1995), pp. 149–162.

41. W. L. Bragg, The diffraction of short electromagnetic waves by a crystal. **17**, 43–57 (1913).

42. E. Widder, Bioluminescence and the Pelagic Visual Environment. *Marine and Freshwater Behaviour and Physiology*. **35**, 1–26 (2002).

43. E. A. Widder, Bioluminescence in the ocean: origins of biological, chemical, and ecological diversity. *Science*. **328**, 704–708 (2010).

44. T. W. Cronin, M. J x000E4 rvilehto, M. Weckstr x000F6 m, A. B. Lall, Tuning of photoreceptor spectral sensitivity in fireflies (Coleoptera: Lampyridae). *Journal of Comparative Physiology A: Sensory, Neural, and Behavioral Physiology*. **186**, 1–12 (2000).

45. W. R. A. Muntz, On yellow lenses in mesopelagic animals. *Journal of the Marine Biological Association of the UK*. **56**, 963–976 (1976).

46. F. de Busserolles *et al.*, Spectral Tuning in the Eyes of Deep-Sea Lanternfishes (Myctophidae): A Novel Sexually Dimorphic Intra-Ocular Filter. *Brain, Behavior and Evolution*. **85**, 77–93 (2015).

47. K. Arikawa, D. G. W. Scholten, M. Kinoshita, D. G. Stavenga, Tuning of Photoreceptor Spectral Sensitivities by Red and Yellow Pigments in the Butterfly Papilio xuthus. *Zoological Science*. **16**, 17–24 (1999).

48. E. A. Widder, M. I. Latz, J. F. Case, MARINE BIOLUMINESCENCE SPECTRA MEASURED WITH AN OPTICAL MULTICHANNEL DETECTION SYSTEM. *The Biological Bulletin*. **165**, 791–810 (1983).

49. P. Jutte, T. Cronin, R. Caldwell, Photoreception in the planktonic larvae of two species of pullosquilla, a lysiosquilloid stomatopod crustacean. *Journal of Experimental Biology*. **201**, 2481–2487 (1998).

50. T. Frank, Comparative study of temporal resolution in the visual systems of mesopelagic crustaceans. *The Biological Bulletin* (1999).

51. F. de Busserolles, N. J. Marshall, Seeing in the deep-sea: visual adaptations in lanternfishes. *Philosophical Transactions of the Royal Society B: Biological Sciences*. **372**, 20160070–9 (2017).

52. K. N. Thomas, B. H. Robison, S. Johnsen, Two eyes for two purposes: in situ evidence for asymmetric vision in the cockeyed squids Histioteuthis heteropsis and Stigmatoteuthis dofleini. *Philosophical Transactions of the Royal Society of London. Series B: Biological Sciences*. **372**, 20160069–9 (2017).

53. S. Johnsen, Hide and Seek in the Open Sea: Pelagic Camouflage and Visual Countermeasures. *Annu. Rev. Marine. Sci.* **6**, 130829112540002 (2013).

54. S. Johnsen, E. A. Widder, C. D. Mobley, Propagation and perception of bioluminescence: factors affecting counterillumination as a cryptic strategy. *Biological Bulletin*. **207**, 1–16 (2004).

55. D.-E. Nilsson, E. J. Warrant, S. Johnsen, R. Hanlon, N. Shashar, A Unique Advantage for Giant Eyes in Giant Squid. *CURBIO*. **22**, 683–688 (2012).

56. R. M. Eakin, J. L. Brandenburger, Differentiation in the eye of a pulmonate snail Helix aspersa. *J. Ultrastruct. Res.* **18**, 391–421 (1967).